Global Solution of Optimization Problems in Rotorcraft Flight Mechanics

Carlo L. Bottasso[1]; Fabio Luraghi[2]; Giorgio Maisano[3]; and Meng Shaohua[4]

Introduction

In rotorcraft flight mechanics, problems such as, for instance, continued and rejected take-off procedures following an engine failure [category A certification (FAA 1999)], optimal auto-rotation, landing procedures after tail-rotor loss, and the analytical, i.e., nonpiloted, simulation of aeronautical design standard-33 (ADS) mission task elements (U.S. AAMD 2000), can be profitably studied with the help of trajectory optimization. In all these cases, the analyst is interested in computing an extremal maneuver for a given vehicle model; one looks for a solution that minimizes a cost function while satisfying given constraints that translate various requirements including the boundaries of the performance envelope of the vehicle. Clearly, the quality of the results strongly depends on the fidelity of the model to the actual vehicle. If flight-test data are available, parameter estimation techniques can be used to tune the model parameters, thereby enhancing the ability of the model to represent the actual vehicle behavior. In this circumstance, the analyst is interested in finding the values of the parameters in the given mathematical model such that the model-computed response best matches (in a statistical sense) the experimentally observed one.

The software system identification and trajectory optimization program (STOP) was developed at the Dipartimento di Scienze e Tecnologie Aerospaziali of the Politecnico di Milano and conceived as a tool to be used in support of certification and formulation of operational procedures for rotorcraft vehicles. STOP has the ability to treat under a common framework both trajectory optimization problems (Bottasso et al. 2010b, 2012), also referred to in the following as maneuver optimal control problems (MOCPs), and parameter estimation problems (PEPs) (Bottasso et al. 2010a). In fact, it can be shown that both can be formulated as two-point boundary value constrained optimization problems defined over a temporal domain of known or unknown duration; moreover, both can be discretized in time using the same techniques, thereby obtaining a constrained nonlinear programming (NLP) problem that is formally identical in the two cases (Bottasso et al. 2009a).

Some of the features of STOP have already been discussed in a series of previous publications by the authors (Bottasso et al. 2009a, 2010a, b). In this work, the authors describe the development of evolutionary algorithms (EAs) (Bäck et al. 1997) for the global solution of MOCPs and PEPs and their integration into STOP (Bottasso et al. 2011b).

This work is motivated by the fact that trajectory optimization problems might lead to NLP problems that are nonconvex and hence with multiple solutions (Luraghi 2009; Celi 2007). In this case, gradient-based methods are likely to converge to local optimal solutions. Furthermore, convergence is often possible only in the presence of suitable initial guesses, whose determination is a sometimes hard and often problem-dependent problem. Therefore, there is a need to develop tools that are capable of effectively exploring the space of solutions, seeking global optima, and reducing the need to generate good quality initial guesses.

Designed to solve nonconvex problems, EAs borrow their working principle from the mechanisms that govern the process of natural evolution of biological organisms. By the application of genetic operators (selection, crossover, mutation), a population of possible solutions (individuals) is allowed to evolve through successive generations so as to promote the individuals that better meet some given design requirements. Since EAs are unconstrained optimization methods, their successful application to the solution of constrained problems requires the use of suitable constraint-handling techniques; a comprehensive survey of the different techniques that have been used to handle constraints in EAs is given in Coello (2002).

[1]Professor, Dipartimento di Scienze e Tecnologie Aerospaziali, Politecnico di Milano, Milano, Italy; and Chair of Wind Energy, Technische Univ. München, Boltzmannstraße 15, 85748 Garching b. München, Germany (corresponding author). E-mail: carlo.bottasso@polimi.it

[2]Engineer, iChrome, Maxet House, 28 Baldwin St., Bristol BS1 1NG, U.K.

[3]Engineer, AWParc, AgustaWestland Politecnico Advanced Rotorcraft Center s.r.l., Via Durando 10, 20100 Milano, Italy.

[4]Ph.D. Candidate, Beijing Univ. of Aeronautics and Astronautics, XueYuan Rd. No. 37, HaiDian District, Beijing, China.

Note. This manuscript was submitted on December 14, 2012; approved on July 10, 2013; published online on July 12, 2013. Discussion period open until October 30, 2014; separate discussions must be submitted for individual papers.

Published works that have investigated the use of EAs for the solution of optimal control problems rely on the use of either penalty functions (Wang and Chiou 1997) or specialized genetic operators (Seren et al. 2006; Onnen et al. 1997). In the former case, one transforms a constrained problem into an unconstrained one by penalizing constraint violations in the objective function with suitably high weights. Despite its simplicity, the major drawback of such an approach is that it requires fine tuning of the penalty parameters, and this might not be a trivial task when dealing with highly-constrained search spaces. The latter approach, in contrast, is more involved: by taking advantage of the knowledge of the constraint conditions imposed on the problem at hand, ad hoc modifications of the genetic operators are introduced to preserve the feasibility of the solutions at all generations. However, this leads to specialized computer codes, i.e., codes capable of solving just one specific problem type. Clearly, this is not desirable when one is interested in developing a tool that can be applied to an ample variety of problems.

The approach proposed in this work makes use of a split of the design variables: a first set (typically represented by model parameter, control policies, and/or initial conditions) is handled by the global EA optimizer, whereas a second set (typically involving state variables but also possibly control inputs, as better explained later on) is handled by a local optimizer using a sequential quadratic programming (SQP) method. When working at the level of vehicle states, the SQP optimizer effectively implements a repair heuristic on these quantities, making them compatible with the problem constraints. Because this can be a time consuming process, the SQP method is typically run only for a limited number of iterations. When achieving a feasible solution within the specified maximum number of iterations proves to be difficult, the repair heuristic is given a limited authority on the control time histories; however, the repaired individual is never returned to the population [never replacing approach (Coello 2002)]. Using a repair technique reduces the search space of EA to feasible solutions only; hence, no special operators or modifications of the objective function need to be considered. Hence, the resulting code can be used to solve the different classes of problems that find applicability in the general area of rotorcraft flight mechanics.

The paper first briefly describes the formulation and solution of optimization problems in rotorcraft flight mechanics, with particular reference to the STOP code. After having formulated MOCPs and PEPs as optimization problems using a single common notation, the architecture of STOP is briefly described. Next, the proposed methodology for the use of EA in the solution of maneuver optimal control problems is illustrated. Finally, the application of the global optimization version of STOP to the solution of engineering problems arising in the context of rotorcraft flight mechanics is presented.

Optimization Problems in Rotorcraft Flight Mechanics

Maneuver Optimal Control Problem

Consider a generic flight mechanics model $\mathcal{M}$ described in terms of the following set of nonlinear differential equations:

$$\boldsymbol{f}(\dot{\boldsymbol{x}}, \boldsymbol{x}, \boldsymbol{u}, \boldsymbol{p}, \boldsymbol{w}, t) = \boldsymbol{0} \tag{1a}$$

$$\boldsymbol{y} = \boldsymbol{h}(\boldsymbol{x}) \tag{1b}$$

where $\boldsymbol{x}$ is the state vector, which groups together the structural dynamics (including states that describe rigid and possibly flexible rotor(s), fuselage, engine, etc.) and aerodynamics states (e.g., dynamic inflow variables), $\boldsymbol{u}$ is the control input vector, $\boldsymbol{p}$ is a set of model parameters, and $\boldsymbol{w}(t)$ models other exogenous inputs and disturbances acting on the system (e.g., gusts and air turbulence). Eq. (1*b*) specifies a set of outputs $\boldsymbol{y}$, which typically represent some vehicle states describing its gross motion or other quantities useful for the analysis of the vehicle dynamics. Finally, the notation $(\cdot) = d(\cdot)/dt$ indicates a derivative with respect to time t.

A general MOCP (Bottasso et al. 2005a, b) for model $\mathcal{M}$ can be formulated as

$$\min_{x,y,u,T} J^{\mathrm{MOCP}}(\boldsymbol{y}, \boldsymbol{u}, T, T_i) \tag{2a}$$

$$\text{subject to } \boldsymbol{f}(\dot{\boldsymbol{x}}, \boldsymbol{x}, \boldsymbol{u}, \boldsymbol{p}^*, \boldsymbol{w}^*, t) = \boldsymbol{0} \tag{2b}$$

$$\boldsymbol{y} = \boldsymbol{h}(\boldsymbol{x}) \tag{2c}$$

$$\boldsymbol{g}(\boldsymbol{x}, \boldsymbol{y}, \boldsymbol{u}, t, T, T_i) \le \boldsymbol{0} \tag{2d}$$

The problem is defined over the interval $\Omega = [T_0, T]$, $t \in \Omega$, where the final time T is typically unknown and must be determined as part of the solution. Specific events might be associated with unknown time instants T_i, $T_0 < T_i < T$ (for example, the jettisoning of part of the cargo or other instantaneous conditions).

In Eq. (2*a*), J^{MOCP} indicates the to-be-optimized cost which, depending on the problem at hand, might account for maneuver duration, control activity, fuel consumption, etc., or some other given function of interest that typically expresses an index of performance of the vehicle.

The maneuver definition is completed by providing a set of problem-dependent equality and inequality constraints [Eq. (2*d*)] which translate the operating envelope of the vehicle, the performance and procedural requirements as dictated by norms and regulations (for example, certification rules), and all other necessary maneuver-defining constraints. These same equations will also typically include initial and/or final conditions on the vehicle states $\boldsymbol{x}$.

Notice that the problem is formulated for fixed values of the model parameters $\boldsymbol{p} = \boldsymbol{p}^*$, where the symbol $(\cdot)^*$ indicates a known assigned value. Similarly, if exogenous inputs are present, these are also known, so that $\boldsymbol{w}(t) = \boldsymbol{w}^*(t)$.

Parameter Estimation Problem

A general PEP for the parametric model $\mathcal{M}(\boldsymbol{p})$ can be formulated as

$$\min_{x,y,p} J^{\mathrm{PEP}}(\boldsymbol{z} - \boldsymbol{y}) \tag{3a}$$

$$\text{subject to } \boldsymbol{f}(\dot{\boldsymbol{x}}, \boldsymbol{x}, \boldsymbol{u}^*, \boldsymbol{p}, \boldsymbol{w}, t) = \boldsymbol{0} \tag{3b}$$

$$\boldsymbol{y} = \boldsymbol{h}(\boldsymbol{x}) \tag{3c}$$

$$\boldsymbol{g}(\boldsymbol{p}) \le \boldsymbol{0} \tag{3d}$$

where $\boldsymbol{z}$ are measurements of the outputs gathered at N discrete sampling time instants t_k during the experimental test

$$\boldsymbol{z}(t_k) = \boldsymbol{y}(t_k) + \boldsymbol{v}(t_k) \tag{4}$$

The available measures are affected by noise $\boldsymbol{v}$ with covariance $\boldsymbol{R}_k = E[\boldsymbol{v}_k \boldsymbol{v}_k^T]$, $E[\cdot]$ being the expected value operator. The presence of measurement noise, together with the possible presence of a

process noise term $\boldsymbol{w}$ for modeling disturbances acting on the system (e.g., air turbulence), makes the problem of a stochastic nature. Hence, the to-be-optimized cost function J^{PEP} is typically a statistical measure of the match between quantities $\boldsymbol{z}$ and model outputs $\boldsymbol{y}$.

A maximum likelihood estimator is obtained by choosing

$$J^{\mathrm{PEP}} = \det(\boldsymbol{R}) \tag{5}$$

where $\boldsymbol{R} = 1/N \sum_{k=1}^{N} \boldsymbol{\nu}(t_k)\boldsymbol{\nu}(t_k)^T$, with $\boldsymbol{\nu}(t_k) = \boldsymbol{z}(t_k) - \boldsymbol{y}(t_k)$. Alternatively, a weighted least squares estimator is obtained if

$$J^{\mathrm{PEP}} = \frac{1}{2}\sum_{k=1}^{N} \boldsymbol{\nu}(t_k)^T \boldsymbol{W} \boldsymbol{\nu}(t_k) \tag{6}$$

where $\boldsymbol{W}$ is a weight matrix. This method can be seen as a particular case of the maximum likelihood method for known measurement noise covariance matrix, $\boldsymbol{W} = \boldsymbol{R}^{-1}$ (Jategaonkar 2006). In the filter error method (Jategaonkar 2006), the system states obtained by integrating model Eq. (3*b*) are corrected by a Kalman filter, whose role is to stabilize the integration around the measurements and to account for the presence of process noise; details are omitted for brevity, but the PEP can still be expressed in a form resembling Eq. (3).

Inequality Eq. (3*d*) enforces possible constraints on the model parameters. Such constraints ensure that the estimated parameters lie within acceptable bounds and do not take at convergence values which are nonphysical.

Notice that in this case the model inputs are known and fixed to the values $\boldsymbol{u}(t_k) = \boldsymbol{u}^*(t_k)$ measured during the experimental test (values in between the sampling instants may be interpolated, if necessary). Similarly, the temporal domain $\Omega = [T_0, T^*]$ is also known.

Rotorcraft vehicles are typically unstable, at least in certain flight conditions, and hence they are usually artificially stabilized by means of a control system. This fact has important consequences on the parameter estimation process and must be explicitly taken into account when formulating estimation methods for such vehicles; further details are given in Bottasso et al. (2010a).

STOP Architecture

The architecture of the STOP program is shown in Fig. 1.

A graphical user interface supports the definition of MOCPs and PEPs. The common thread between the solution of the two classes of problems is the discretization in the temporal domain. STOP implements the so-called *direct* approach (Betts 2001), which leads to a nonlinear constrained optimization problem that writes

$$\min_{\boldsymbol{\pi}} J^{\mathrm{NLP}}(\boldsymbol{\pi}) \tag{7a}$$

$$\text{subject to } \boldsymbol{a}(\boldsymbol{\pi}) = \boldsymbol{0} \tag{7b}$$

$$\boldsymbol{b}(\boldsymbol{\pi}) \leq \boldsymbol{0} \tag{7c}$$

where $\boldsymbol{\pi}$ is a set of algebraic unknowns (design variables), and J^{NLP} is a scalar objective function which represents an approximation of the cost of Eq. (2*a*) or (3*a*). The equality constraints in Eq. (7*b*) are generated by the discretization of the equations of motion Eq. (2*b*) or (3*b*), whereas the inequality constraints in Eq. (7*c*) are generated by the discretization of Eq. (2*d*) or (3*d*).

Three discretization techniques are available in STOP—namely, the direct transcription and multiple shooting methods (Bottasso et al. 2010b) and the recently developed hybrid single-multiple shooting (Bottasso et al. 2012). Bottasso et al. (2009a) proposes a classification of optimal areas of applicability of these methods and, for each one of them, derives the specific form of the vector of design variables.

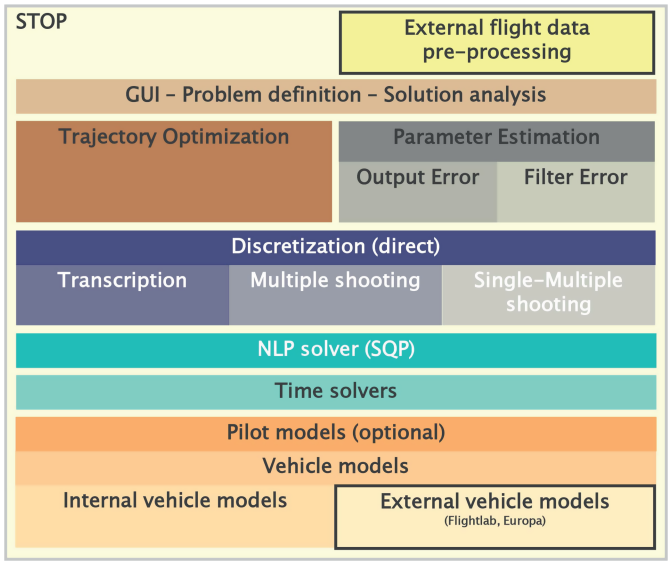

Fig. 1. Architecture of the STOP code (reprinted from Bottasso et al. 2011, with permission)

Time marching can be based either on algorithms available in external vehicle models or with built-in explicit or implicit time solvers.

The vehicle models include an optional layer that models the pilot, which is useful in certain MOCP applications for computing maneuvers considering pilot-in-the-loop effects (Bottasso et al. 2009b). The vehicle itself can be simulated using an internal model or by external codes through a generic interface which supports all necessary operations.

Global Solution of MOCPs and PEPs

In this section, a formulation that makes use of EAs for the solution of problem (7) in the context of MOCPs and PEPs is developed. For a general introduction to EA, the authors refer to Bäck et al. (1997) for a general introduction to EA, to Betts (2001) for optimal control and to Jategaonkar (2006) for parameter estimation.

When using EAs, the computational cost is proportional to the population size. In general, if the population size is too small, then EA might not be able to thoroughly explore the solution space; conversely, increasing the population size generally enables EA to obtain better results. However, it is clear that the larger the population size, the longer it takes EA to compute each generation. As a rule of thumb, population size is usually set to 5–10 times the number of design variables (Bäck et al. 1997).

In light of these considerations, for the solution of optimal control problems using EA in rotorcraft flight mechanics, the use of shooting methods is favored over direct transcription ones because the latter tend to generate potentially large NLP problems (Bottasso et al. 2009a). However, even in this case, there might be a problem of possibly overwhelming computational cost. In fact, when using shooting methods, the problem unknowns are defined as the discrete values of the states at the interfaces between shooting segments, the discrete values of the controls within each segment, and possibly the final time. Thus, one would need to consider extremely large populations to cover all possible feasible values of the design variables.

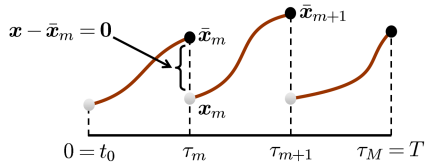

Fig. 2. Basic principle of the multiple shooting method (reprinted from Bottasso et al. 2011, with permission)

As shown in Fig. 2, when the multiple shooting method is used, the time domain Ω is partitioned as $T_0 \equiv t_0 < t_1 < \cdots < t_m < \cdots < t_M \equiv T$ with $\Omega^m = [t_m, t_m + 1]$, $m = (0, M - 1)$, where each Ω^m is a shooting segment. Next, the vehicle equations of motion are marched forward in time within each shooting segment Ω^m, starting from the initial conditions provided by the value of the states x_m at the left boundary of the segment. Segments are then glued together by imposing the equality constraints $x_m - \bar{x}_m = 0$, $m = (1, M)$).

Since EAs can tackle only unconstrained optimization problems, another challenging task in the framework of EAs is the satisfaction of the gluing constraints on the states, which ensure the continuity of their time history across the boundaries of the shooting segments (Fig. 2), and of all other problem constraints

To address these issues, a procedure based on a split of the design variables is proposed: EA is used to compute an optimal solution in terms of the sole controls and/or initial conditions, whereas the feasibility of the computed solution is ensured through the use of a repair heuristic (RH) (Coello 2002).

The solution of a MOCP proceeds as follows. First, the temporal domain $\Omega = [T_0, T]$ is partitioned into N intervals $T^i = [t_i, t_{i+1}]$ of size h^i, $i = (0, N - 1)$. Typically uniform grids are considered and hence, $h^i = h = (T - T_0)/N$. A computational grid $\mathcal{T}_h^{\mathrm{EA}}$ is associated with this partition.

Next, for every individual in the population, depending on the problem at hand, the set of design variables is chosen to include one or more of the following quantities: (1) all values of the controls at the nodes of $\mathcal{T}_h^{\mathrm{EA}}$, and (2) the problem's initial conditions (if free), possibly the final time (if unknown). To limit the population size, coarse temporal grids are considered, i.e., with a reduced number of nodes.

Remark 1

Evolution strategies (ESs) (Beyer and Schwefel 2002) use a representation (encoding) of the design variables as real numbers. The authors have observed that in the case of MOCPs, where very small variations in the controls or in the maneuver duration typically result in small (negligible) variations in the objective function, such encoding might lead to the premature stop of the algorithm because of an excessively low diversity of the individuals in the population. The authors have found that this problem is somehow alleviated by decreasing the resolution with which EA explores the solution space, which can be achieved by forcing the problem unknowns to take only values specified at a small number of equidistant points between their lower and upper bounds. For the generic variable π_i lying in the interval $I_{\pi_i} = [\pi_i^{\min}, \pi_i^{\max}]$, the set Π_i of admissible values is constructed as $\Pi_i = \{\pi_i^{\min} + j\Delta\pi_i, j = 0, \ldots, L\}$, with $L = (\pi_i^{\max} - \pi_i^{\min})/\Delta\pi_i$, where $\Delta\pi_i$ is the resolution of the discretization of I_{π_i}. This turns the original problem into a discrete combinatorial optimization problem.

Controls computed by EA are then projected onto a finer grid $\mathcal{T}_h^{\mathrm{RH}}$, associated with a partition of Ω into M shooting segments and a suitable discretization of the controls within each segment. This projection can be expressed with the notation

$$\boldsymbol{u}|_{\mathcal{T}_h^{\mathrm{RH}}} = \mathcal{P}(\boldsymbol{u}|_{\mathcal{T}_h^{\mathrm{EA}}}) \tag{8}$$

where $\mathcal{P}(\cdot)$ is an appropriate projection operator. The time history of vehicle states that are compatible with the given control policy and maneuver-defining constraints is found from the solution of the following NLP problem:

$$\min_{\boldsymbol{\theta}} K(\boldsymbol{\theta}, \boldsymbol{u}|_{\mathcal{T}_h^{\mathrm{RH}}}) \tag{9a}$$

$$\text{s.t. } \boldsymbol{g}(\boldsymbol{\theta}, \boldsymbol{u}|_{\mathcal{T}_h^{\mathrm{RH}}}) = \boldsymbol{0} \tag{9b}$$

$$\boldsymbol{\theta} \in [\boldsymbol{\theta}^{\min}, \boldsymbol{\theta}^{\max}] \tag{9c}$$

where the unknowns $\boldsymbol{\theta}$ are the values of the states at the interfaces between shooting segments. Objective function K represents a measure (in a given norm) of the violation of constraints (7*b*) and (7*c*) expressed in terms of $\boldsymbol{\theta}$ and $\boldsymbol{u}|_{\mathcal{T}_h^{\mathrm{RH}}}$, whereas Eq. (9*b*) represents the gluing constraints, which are evaluated by marching the vehicle equations of motion forward in time under the action of the controls $\boldsymbol{u}|_{\mathcal{T}_h^{\mathrm{RH}}}$. Problem (9) is solved using a SQP method with Jacobians computed through centered finite differencing by perturbation of the unknowns (Barclay et al. 1997).

Finally, cost J^{NLP} of Eq. (7*a*) is evaluated using the computed time histories of the states and corresponding outputs within each shooting segment.

Remark 2

Solving problem (9) might be a time consuming process and hence the SQP method is typically run only for a limited number of iterations. When achieving a feasible solution within the specified maximum number of iterations is difficult, RH is allowed a limited authority on the inputs by modifying the given control time history as

$$\boldsymbol{u}|_{\mathcal{T}_h^{\mathrm{RH}}} + \Delta\boldsymbol{u}|_{\mathcal{T}_h^{\mathrm{RH}}} \tag{10}$$

where $\Delta\boldsymbol{u}|_{\mathcal{T}_h^{\mathrm{RH}}}$ are bounded corrective terms, i.e., $\Delta\boldsymbol{u}|_{\mathcal{T}_h^{\mathrm{RH}}} \in [\Delta\boldsymbol{u}^{\min}, \Delta\boldsymbol{u}^{\max}]$, that are computed as part of the solution to problem (9). However, the repaired individuals are never returned to the population [never replacing approach (Coello 2002)].

The solution of PEPs can be developed along similar lines, although things are simpler in this case given the fact that control inputs are known. Therefore, the global optimizer operates at the level of the model parameters, whereas the local optimizer is used for the satisfaction of the gluing constraints at the interface between shooting arcs.

Numerical Applications

In this section, the application of STOP is presented, equipped with the proposed global optimization procedure, to the solution of problems arising in the context of rotorcraft flight mechanics applications.

Vehicle model equations are derived based on three-dimensional rigid body dynamics. Rotor forces and moments are computed analytically by combining actuator disk and blade element theory, considering a uniform inflow (Prouty 1990). The rotor attitude is evaluated by means of quasi-steady flapping dynamics with a linear aerodynamic damping correction. Look-up tables are used for the quasi-steady aerodynamic coefficients of the vehicle lifting surfaces, and simple corrections for compressibility effects and for the downwash angle at the tail because of the main rotor are

included in the model. Further details on the model structure are given in Bottasso et al. (2005b) and Maffezzoli (2009).

Design of Optimal Inputs for Parameter Estimation of a Small Autonomous Helicopter

The design of globally optimal input signals for parameter estimation flight trials is considered. This example is chosen here because it combines the characteristics of a MOCP with those of a PEP. In fact, in this case, the idea is to formulate a MOCP that maximizes the identifiability of a given set of parameters in the vehicle model.

Multistep inputs are commonly used input signals during flight tests for parameter estimation. They consist of a sequence of alternating positive and negative amplitude pulses with different duration. In this case, the design problem consists in finding the optimal amplitude and width of the pulses so that the information content in the experimental data, as embodied in the Fisher information matrix (Kullback 1959), is maximized. Therefore, for this problem the EA optimization variables are represented by the control inputs, whereas the SQP optimizer is used for compatibilizing the vehicle states. Solutions are obtained with the self-adaptive EA implemented in the commercial software *OPTIMUS*.

A small-size rotorcraft unmanned aerial vehicle (RUAV) is considered; the test condition is a forward level flight at a very low advance ratio, $\mu = 0.04$ ($V = 5$ m/s). Only the longitudinal dynamics of the vehicle is considered. The analysis starts from the controls set to their trim values and perturb the main rotor longitudinal cyclic, while holding the others fixed. Control perturbations are restricted to lie in the interval $I_A = [-1, 1]$ deg. For such an experiment, the model parameters of principal interest are the main rotor aerodynamic coefficients—namely, the rotor blade lift curve slope C_{L_α} and mean drag C_D. Interval I_A is discretized with a resolution of 0.25 deg and the population size is set to 100.

The computed optimal input is shown in Fig. 3 using a solid line; the same figure also shows using a dashed-dotted line the DLR 1-1-2-3 input, a widely known input form that has been shown to be very effective for flight vehicle parameter estimation (Jategaonkar 2006). Table 1 gives the results of the maximum likelihood estimation of the main rotor aerodynamic parameters for the optimal multistep and the 1-1-2-3 inputs. Although the latter

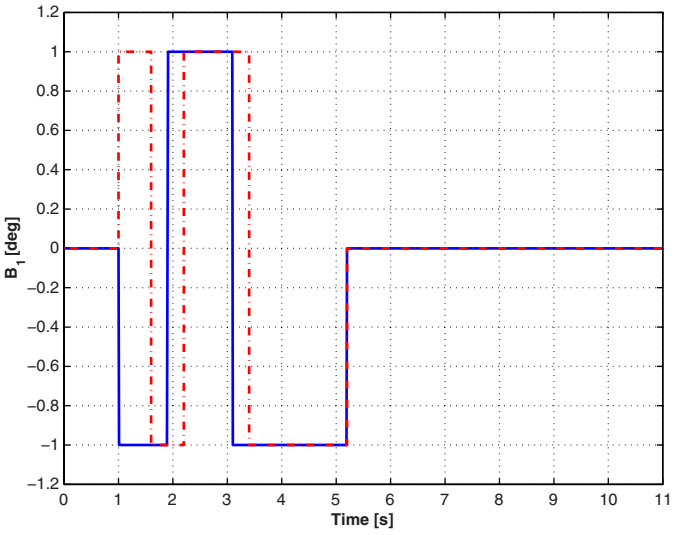

Fig. 3. Optimal longitudinal cyclic input (solid line) and 1-1-2-3 input (dash-dotted line) (reprinted from Bottasso et al. 2011, with permission)

Table 1. Estimated Value and Standard Deviation of Main Rotor Aerodynamic Parameters for 1-1-2-3 and Optimal Longitudinal Cyclic Inputs

	1-1-2-3		Optimal multistep	
Parameter	Estimated value	Standard deviation	Estimated value	Standard deviation
$C_{L_{\alpha_{MR}}}$ [rad^{-1}]	5.62012	0.00576	5.61134	0.00472
$C_{D_{MR}}$	0.00974	0.00034	0.00973	0.00033

was carefully tuned to excite the vehicle longitudinal natural frequencies (Maffezzoli 2009), the accuracy of the estimate of the blade lift curve slope is increased by 18% when using the optimized input.

Category A Continued Take-Off Maneuver for a Medium-Size Helicopter

In this section, the take-off maneuver for a 10 ton twin-engine four-bladed helicopter under category A certification requirements (FAA 1999) is considered, which ensure a safe behavior of the vehicle even after an engine failure. Such an emergency maneuver was previously studied in Bottasso et al. (2005a, b).

Normally a category A continued take-off is flown in a vertical plane. Following the loss of power during a climb towards or in hover at the take-off decision point (TDP), the vehicle is aggressively pitched forward to gain speed. As the vehicle starts falling while gaining forward speed, its necessary power is reduced; this in turn can be used to slow down the descent, to bring the rotor speed back to its nominal value and eventually to start climbing and regain altitude.

In this paper, the authors want to investigate whether a more three-dimensional maneuver than the classical one can be used to reduce the loss of altitude following an engine loss. In fact, since the vehicle roll inertia is much lower then the pitch one, it can be hypothesized that one could more rapidly gain speed and hence, reduce necessary power by rolling sideways than by the classical forward pitching. Because the helicopter, as far as its flight mechanics characteristics are concerned, is a nonsymmetric vehicle with respect to its longitudinal plane, rolling right or left will have different effects, which also should be understood.

To investigate this problem, different initial conditions in terms of climb velocity W, horizontal velocity U and heading angle ψ are considered. Heading is measured with respect to the vertical plane containing the vehicle velocity vector at the end of the maneuver, the so-called take-off safety speed V_{TOSS} (FAA 1999).

For a null heading, the vehicle is initially aligned with the plane containing the final climb. Even in this case, the vehicle is free to sideslip throughout the maneuver and hence rotate out of the maneuver-containing plane if necessary to reduce the loss of altitude. This is in fact what is typically observed, as shown in Fig. 4 for an optimal maneuver starting in hover at the TDP; this result is not surprising because helicopters do not exhibit a symmetric behavior with respect to their longitudinal plane.

Conversely, for a nonnull initial heading, the vehicle will not only pitch forward but also roll sideways and then finally rotate so as to align itself with the climb plane. A typical trajectory is visualized in Fig. 5 for a case where the power loss takes place during the climb to the TDP; after an aggressive lateral roll to quickly accelerate and decrease necessary power, the vehicle rotates before starting to climb and regain altitude. Clearly, the significant initial sideslipping and nonnull heading also have an

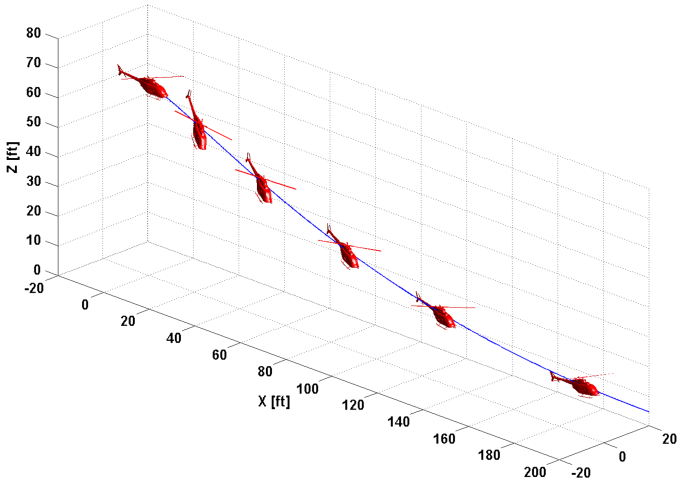

Fig. 4. Sideslipping but mostly planar trajectory for a continued take-off

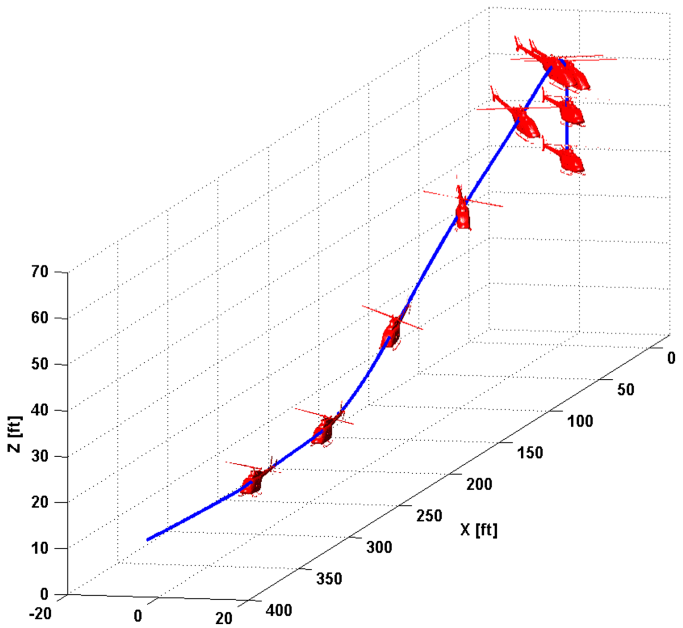

Fig. 5. Three-dimensional maneuver for a continued take-off, with initial roll followed by realignment

impact on the pilot visibility, whose effects are, however, not considered here for simplicity.

In this case, the EA optimization variables are represented by the initial conditions, and the SQP optimizer deals with control inputs, vehicle states, and maneuver duration. Solutions are computed with the self-adaptive EA implemented in the commercial software *NEXUS* (iChrome 2012).

Two different global optimization runs were performed. In the first case, only negative initial headings are considered, and the search region for the three EA variables is within the following ranges:

$$U \in [-2, 0] \text{ KTS} \tag{11a}$$

$$W \in [-5, 0] \text{ KTS} \tag{11b}$$

$$\psi \in [-45, 0] \text{ deg} \tag{11c}$$

with a resolution of 1 KT for the velocities and 5 deg for the heading angle.

The optimization cost function accounts for the control input rates and the initial vertical position H (TDP altitude), i.e., it reads

$$J^{\text{MOCP}} = H + \frac{1}{T}\int_T \dot{\boldsymbol{u}} \cdot \boldsymbol{W}\dot{\boldsymbol{u}} dt \tag{12}$$

The principal optimization constraints include the minimum rotor speed that should not fall below 90% of the nominal revolutions per minute (RPM) value, a ground clearance not less than 15 ft, and a minimum pitch angle not exceeding -10 deg. The exit conditions include a climb velocity of 100 ft/ min, the rotor speed back to 100%, and null angular velocities. The starting guess is provided by a previously calculated STOP solution with a heading of -45 deg and null vertical and horizontal velocity components.

Results in terms of minimum altitude H versus heading ψ, vertical velocity W, and backup speed U are plotted in Fig. 6 from top to bottom, respectively. Each point in the graphs represents an individual in the population generated by the EA solver. The optimal solution uses the maximum available climb velocity, a null horizontal speed (i.e., vertical climbing), and a heading of 35 deg.

This problem nicely illustrates the danger of remaining trapped in a local minimum when using local optimizers. In fact, the same problem was solved again using SQP, for $U = 0$ KTS, $W = -5$ KTS (the global optimum values), and with an initial heading constrained between 0 and -45 deg. The converged SQP solution has an initial heading of -45 deg, which, however, exhibits a higher associated TDP. This means that the EA solution is a lower minimum than the one found by SQP.

To better illustrate the possible presence of local minima in this unusual optimal control problem, the category A optimization was repeated again. The range of initial yaw angles was set to be between -45 deg and 45 deg, with a resolution of 1 deg, whereas the velocity components were held fixed at their global optimum values ($U = 0$ KTS, $W = -5$ KTS). Furthermore, the heading angle was added to the cost function to try to reduce it because pilots typically prefer to work with a small sideslip (which improves visibility), resulting in the new cost

$$J^{\text{MOCP}} = H + \frac{1}{T}\int_T (\dot{\boldsymbol{u}} \cdot \boldsymbol{W}\dot{\boldsymbol{u}} + w_\psi \psi^2) dt \tag{13}$$

The results, illustrated in Fig. 7 in terms of TDP altitude versus initial heading, show that there is a global optimum at -43 deg and local optima at 23 and 31 deg. Some scatter of the points in the plots is because of generous tolerances in the solution of the SQP problems. The authors remark that any point in the plots is a solution for the local optimizer, which again highlights the potential danger of being trapped in a local minimum when using nonglobal optimization algorithms.

These plots confirm the initial hypothesis. If one flies a standard continued take-off, corresponding to the case $\psi = 0$, the loss of altitude is of approximately 39 ft. Conversely, rolling left and climbing at approximately 40 deg from the initial heading gives a much better performance, reducing the loss of altitude to only approximately 32 ft. On the contrary, if one were to roll right and then realign, the performance would be initially worsened, reaching approximately 41 ft at 15 deg, although then it would improve again to approximately 38 ft for 30 deg of realignment.

In summary, it appears that the minimum possible loss of altitude would be obtained not by a fast forward pitching, as classically done, but by a sideways rolling on a specific side of the vehicle that,

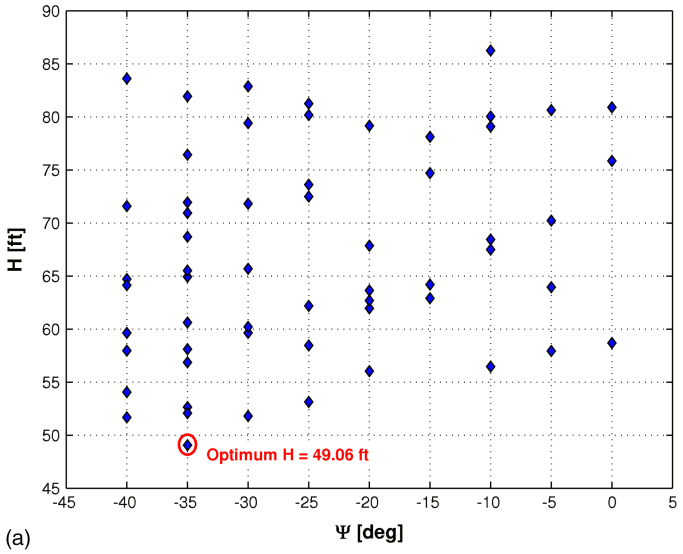

(a)

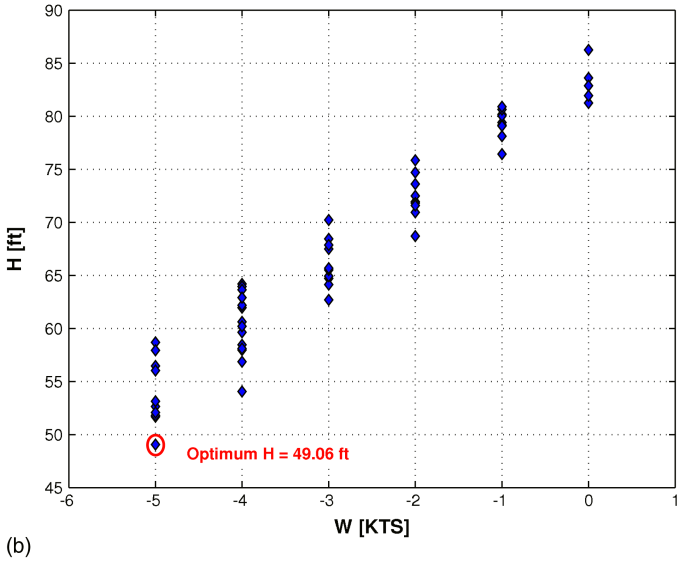

(b)

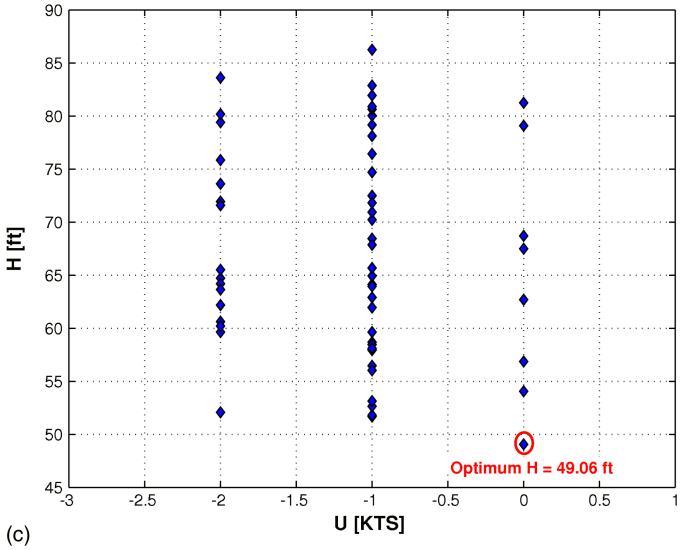

(c)

Fig. 6. Category A continued take-off; Minimum altitude H, vertical velocity W, and horizontal speed U versus heading ψ: (a) minimum altitude H; (b) vertical velocity W; (c) horizontal speed U (reprinted from Bottasso et al. 2011, with permission)

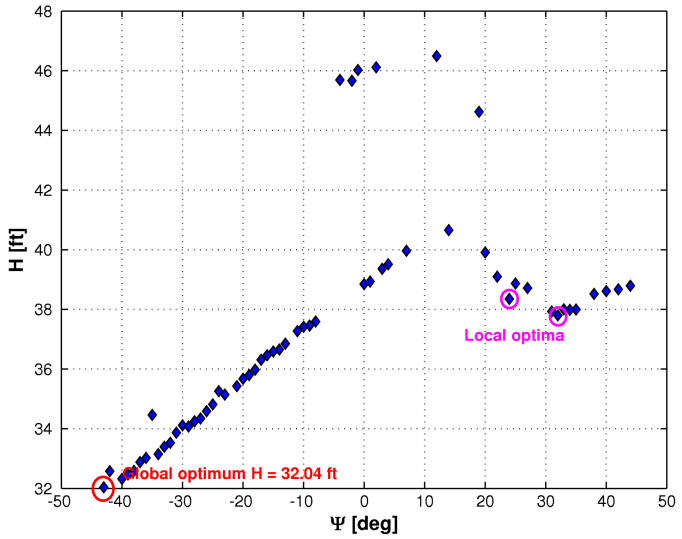

Fig. 7. Category A continued take-off; TDP altitude versus initial heading angle ψ (reprinted from Bottasso et al. 2011, with permission)

exploiting the reduced inertia about the roll axis, is capable of accelerating faster and hence reduces necessary power in a shorter amount of time. This of course would have to be traded against a more complex maneuver with possible visibility issues.

Height-Velocity Diagram for a Light Rotorcraft

The height-velocity (H-V) diagram of a vehicle represents the performance for a safe landing maneuver under a power failure condition, and it indicates an area in the height-velocity plane that should be avoided. To trace the H-V diagram of a given vehicle, test pilots fly a large number of different flight conditions during the certification of the aircraft. Because this is a time consuming operation, the numerical identification of the safe H-V boundaries is attractive to potentially reduce the number of necessary flight trials. In this section, the H-V diagram for a light rotorcraft is first determined, and then the most dangerous region where operating the vehicle within this unsafe area is investigated.

Two different optimization runs were performed. In the first case, the minimum initial flight speed that still allows for a safe landing maneuver is computed. The corresponding MOCP is formulated as

$$J^{\mathrm{MOCP}} = U + \frac{1}{T}\int_T \dot{\boldsymbol{u}} \cdot \boldsymbol{W}\dot{\boldsymbol{u}}dt \tag{14}$$

where U is the initial velocity that should be minimized, subjected to constraints ensuring safe impact velocities that are compatible with the energy absorption capacity of the vehicle, which were chosen as

$$U_T \leq 10 \text{ KTS} \tag{15a}$$

$$W_T \leq 2 \text{ KTS} \tag{15b}$$

The initial altitude H is allowed to vary within the range $H \in [10{,}130]$ ft. For all simulations, the initial conditions correspond to a steady level flight. Furthermore, throughout the duration of the maneuver, the rotor speed should not fall below 90% of its nominal value, and negative pitch should not exceed -10 deg.

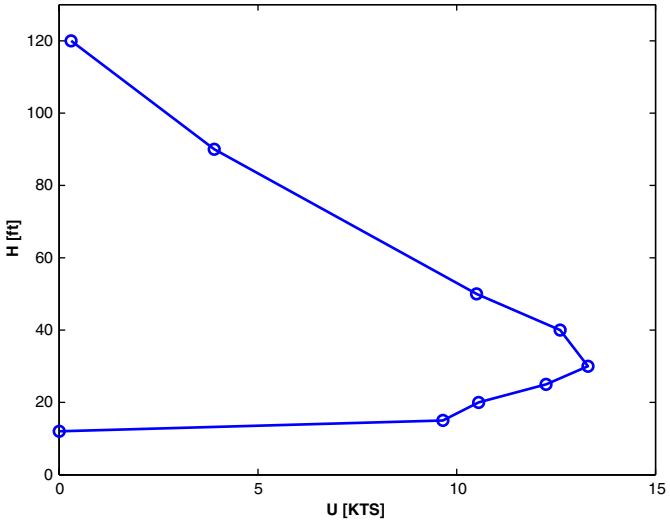

Fig. 8. H-V diagram for a light helicopter

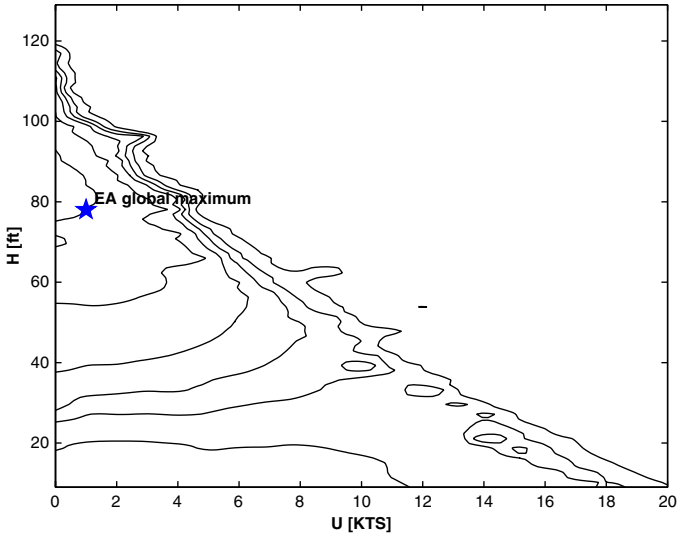

Fig. 9. Isocontour plot of cost function for exhaustive search procedure

Fig. 8 shows the obtained H-V curve which exhibits the expected trend. At relatively low speeds, safe landing is possible either for low altitudes (because of low potential energy) or at higher ones (because there is enough time to make use of the autorotation capabilities of the vehicle to slow down its descent). However, the intermediate altitudes are unsafe and should be avoided in operation.

Nonetheless, there are situations where it is impossible for the accomplishment of particular missions to completely avoid the unsafe regions of the H-V plane. Therefore, it becomes necessary to know what combinations of airspeed and altitude are the most dangerous.

To study this problem, an EA optimization was performed. Given flight altitude and speed, an optimal maneuver is sought to land the vehicle with minimum impact velocity, an effect which was translated into the following MOCP cost function:

$$J^{\text{MOCP}} = w_U U_T^2 + w_W W^2 + \frac{1}{T}\int_T (\dot{\boldsymbol{u}} \cdot \boldsymbol{W}\dot{\boldsymbol{u}} + w_P \dot{P}^2)dt \qquad (16)$$

where U_T and W_T are landing velocity components, P power, and w_U, w_W and w_P are cost weighting factors. In this case, the EA optimization variables are the initial forward speed and altitude, whereas all other constraints are the same as in the previous case. STOP handles control inputs, vehicle states, and maneuver duration, and solutions are computed with the *NEXUS* optimization environment. The search region for the EA variables was set as follows:

$$U \in [0, 20] \text{ knots} \qquad (17a)$$

$$H \in [10{,}100] \text{ knots} \qquad (17b)$$

with a resolution of 1 knot for the horizontal speed and 3 ft for height. As the objective is to find the maximum landing velocities according to different combinations of initial altitude and airspeed, the to-be-maximized EA cost function is defined as

$$J^{\text{MOCP}} = w_U U_T^2 + w_W W^2 \qquad (18)$$

which in this way identifies the criticality of the landing maneuver. In fact, the higher the touch-down velocities, the more dangerous it is to land the vehicle.

To prove that the optimum solution found by the EA optimizer is global, an exhaustive search procedure was implemented by computing all points in the H-V plane corresponding to the resolution of the EA optimization. The resulting isocontour of the EA objective value is plotted in Fig. 9. The picture shows the level of dangerousness of various regions in the H-V plane. It appears that danger increases rather steeply when moving within the to-be-avoided area from the upper branch of the curve, i.e., moving down from the higher altitudes. On the other hand, danger increases in a milder manner while moving up from the lower altitudes. The global maximum, i.e., the most dangerous condition associated with the highest landing speeds, corresponds to 78 ft of initial altitude and 1 KT of initial horizontal speed. The global maxima found by the exhaustive search procedure and by the EA optimizer (marked in the same plot) are almost identical. However, the maximum was found by the EA optimizer solving only 280 MOCPs, whereas the exhaustive search considered 861 different MOCPs, with a substantial difference in computational cost.

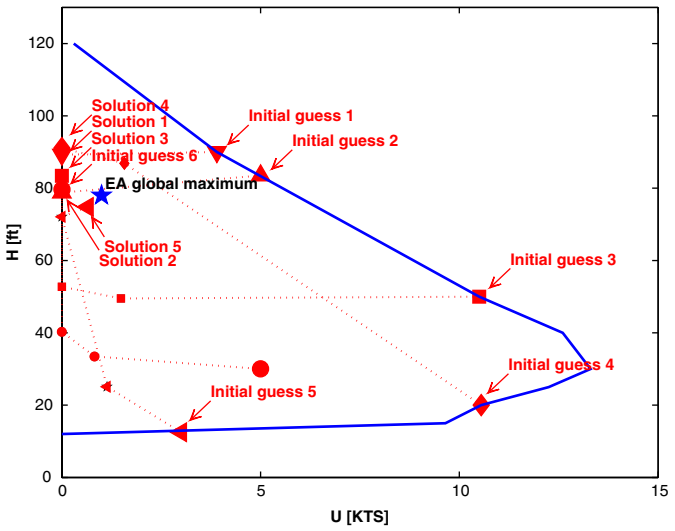

Fig. 10. Trapping of the SQP approach in local maxima

The same problem was repeated using the nonlinear constrained SQP optimization algorithm which, compared to the EA optimizer, is very sensitive to initial guesses and has the potential of being trapped in local optima. To illustrate this problem, SQP optimization was initiated from six different starting points in the H-V plane. The results are illustrated in Fig. 10 which shows the six initial conditions and the six paths towards the six associated converged results. It appears that only one of the optimizations approximately arrived at the global maximum, whereas the other five were trapped in local maxima, often quite far away from the global one.

Conclusions

In this paper, a numerical procedure was presented for the global solution using evolutionary algorithms of trajectory optimization problems in rotorcraft flight mechanics. Based on experience, local optima are usually not a major issue for many flight mechanics optimization problems, in the sense that one is typically able to compute solutions of engineering interest by simply using gradient-based methods. However, as the applicability of such techniques to a variety of rotorcraft flight mechanics problems is progressively expanded, it becomes important to guarantee that one is not missing relevant and better solutions. Furthermore, a well-performing global optimizer reduces the need of generating good quality initial guesses, which is sometimes hard and is often a problem dependent issue.

The proposed approach makes use of a global EA coupled to a repair heuristic which ensures the feasibility of the computed solution. Using a repair heuristic reduces the EA search space to feasible solutions only; hence, no special evolutionary operators or modifications of the objective function need to be considered. This way, the resulting code can be used to solve different classes of optimization problems, including optimal control and parameter estimation ones.

Three different application problems have been used for demonstrating the proposed methodology. In the first, a control input time sequence for identification trials of a small unmanned helicopter that improves the commonly adopted 1-1-2-3 signal has been designed. In the second, a new strategy for flying category A continued take-offs has been designed that improves on the standard mostly planar maneuvers; such result was obtained by solving maneuver optimal control problems that present multiple local minima. In the third, the H-V diagram of a helicopter was first traced, and then the most dangerous condition within the to-be-avoided unsafe domain was identified, showing here again the fact that standard gradient-based approaches can be trapped in local stationary points.

The applications proposed in this work constitute preliminary results that, however, allow one to draw some conclusions. In particular, they suggest that the coupling of a global optimizer like EA with a local optimizer based on SQP allows one to effectively explore the space of solutions. Typically, for this to work, one has to avoid conflicts between the two optimizers, which therefore work on different sets of variables: a small set that includes control inputs, model parameters, initial conditions, etc., for the global optimizer, and the remaining set for the local optimizer, which is in charge of satisfying all nonlinear constraints.

Acknowledgments

The second author wishes to thank Professor R. Celi for the stimulating discussions on the use of evolutionary algorithms for the solution of optimization problems, during his stay at the Department of Aerospace Engineering of the University of Maryland, College Park, MD.

References

Bäck, T., Fogel, D., and Michalewicz, Z., eds. (1997). *Handbook of evolutionary computation*, Oxford University Press, New York.

Barclay, A., Gill, P. E., and Rosen, J. B. (1997). "SQP methods and their application to numerical optimal control." *Rep. NA 97-3*, Dept. of Mathematics, Univ. of California, San Diego.

Betts, J. T. (2001). *Practical methods for optimal control using non-linear programming*, Society for Industrial and Applied Mathematics (SIAM), Philadelphia.

Beyer, H.-G., and Schwefel, H.-P. (2002). "Evolution strategies: A comprehensive introduction." *Nat. Comput.*, 1(1), 3–52.

Bottasso, C. L., Croce, A., Leonello, D., and Riviello, L. (2005a). "Optimization of critical trajectories for rotorcraft vehicles." *J. Am. Helicopter Soc.*, 50(2), 165–177.

Bottasso, C. L., Croce, A., Leonello, D., and Riviello, L. (2005b). "Rotorcraft trajectory optimization with realizability considerations." *J. Aerosp. Eng.*, 10.1061/(ASCE)0893-1321(2005)18:3(146), 146–155.

Bottasso, C. L., Luraghi, F., Maffezzoli, A., and Maisano, G. (2010a). "Parameter estimation of multibody models of unstable systems from experimental data, with application to rotorcraft vehicles." *J. Comput. Nonlinear Dyn.*, 5(3), 031010.

Bottasso, C. L., Luraghi, F., and Maisano, G. (2009a). "A unified approach to trajectory optimization and parameter estimation in vehicle dynamics." *Proc., CMND 2009, Int. Symp. on Coupled Methods in Numerical Dynamics*, Univ. of Zagreb, Zagreb, Croatia.

Bottasso, C. L., Luraghi, F., and Maisano, G. (2011). "On an integrated software tool in support of certification and formulation of operational procedures for rotorcraft vehicles." *Proc., 37th European Rotorcraft Forum*, European Rotorcraft Forum (ERF).

Bottasso, C. L., Luraghi, F., and Maisano, G. (2012). "Efficient rotorcraft trajectory optimization using comprehensive vehicle models by improved shooting methods." *Aerosp. Sci. Technol.*, 23(1), 34–42.

Bottasso, C. L., Maisano, G., and Scorcelletti, F. (2009b). "Trajectory optimization of rotorcraft including pilot models, with applications to ADS-33 MTEs, Cat-A procedures and engine off-landings." *Proc., AHS 65th Annual Forum and Technology Display*, American Helicopter Society, Alexandria, VA.

Bottasso, C. L., Maisano, G., and Scorcelletti, F. (2010b). "Trajectory optimization procedures for rotorcraft vehicles, their software implementation, and applicability to models of increasing complexity." *J. Am. Helicopter Soc.*, 55(3), 032010.

Celi, R. (2007). "Analytical simulation of ADS-33 mission task elements." *Proc., American Helicopter Society (AHS) 63rd Annual Forum and Technology Display*, American Helicopter Society, Alexandria, VA.

Coello, C. A. (2002). "Theoretical and numerical constraint-handling techniques used with evolutionary algorithms: A survey of the state of the art." *Comput. Methods Appl. Mech. Eng.*, 191(11–12), 1245–1287.

Federal Aviation Administration (FAA). (1999). *Advisory Circular 29-2C, Certification of Transport Category Rotorcraft*, Dept. of Transportation, Washington, DC.

iChrome. (2012). "NEXUS." ⟨http://ichrome.com/nexus/overview⟩ (Apr. 14, 2014).

Jategaonkar, R. V. (2006). *Flight vehicle system identification. A time-domain approach*, American Institute of Aeronautics and Astronautics (AIAA) Progress in Astronautics Aeronautics, Reston, VA.

Kullback, S. (1959). *Information theory and statistics*, Wiley, New York.

Luraghi, F. (2009). "Time-domain parameter estimation techniques for first-principle rotorcraft models." Ph.D. thesis, Politecnico

di Milano, Dipartimento di Ingegneria Aerospaziale, Milano, Italy.

Maffezzoli, A. (2009). "Procedures for the estimation of model parameters for a small rotorcraft UAV." M.Sc. thesis, Politecnico di Milano, Dipartimento di Ingegneria Aerospaziale, Milano, Italy.

Onnen, C., Babuška, R., Kaymak, U., Sousa, J. M., Verbruggen, H. B., and Isermann, R. (1997). "Genetic algorithms for optimization in predictive control." *Control Eng. Pract.*, 5(10), 1363–1372.

OPTIMUS, optimization environment, version 5.3 [computer software]. Noesis Solutions, Leuven, Belgium.

Prouty, R. W. (1990). *Helicopter performance, stability, and control*, R.E. Krieger Publishing, Malabar, FL.

Seren, C., Bommier, F., Bucharles, A., Verdier, L., and Alazard, D. (2006). "Flight test protocol optimization using genetic algorithms." *Proc., 14th Int. Federation of Automatic Control (IFAC) Symp. on System Identification*, International Federation of Automatic Control (IFAC), Laxenburg, Austria.

U.S. Army Aviation and Missile Command (U.S. AAMD). (2000). "Handling qualities requirements for military rotorcraft aeronautical design standard." *Rep. ADS-33E-PRF*, Aviation Engineering Directorate, Redstone Arsenal, AL.

Wang, F. S., and Chiou, J. P. (1997). "Optimal control and optimal time location problems of differential-algebraic systems by differential evolution." *Ind. Eng. Chem. Res.*, 36(12), 5348–5357.